frontiers | Frontiers in Materials

TYPE Original Research
PUBLISHED 21 February 2023
DOI 10.3389/fmats.2022.1025830

OPEN ACCESS

EDITED BY
Neven Ukrainczyk,
Darmstadt University of Technology, Germany

REVIEWED BY
Suvash Chandra Paul,
International University of Business Agriculture and Technology, Bangladesh
Peng Zhang,
Zhengzhou University, China

*CORRESPONDENCE
Baojun Zhao,
2235571847@qq.com

SPECIALTY SECTION
This article was submitted to Structural Materials, a section of the journal Frontiers in Materials

RECEIVED 23 August 2022
ACCEPTED 29 September 2022
PUBLISHED 21 February 2023

CITATION
Zhao B, Zhang Z, Wu C, Zou C, Xu X, Yang H and Zhang W (2023), An ultra-high performance concrete incorporating viscosity-controlling agent: Fiber distribution and microstructure.
Front. Mater. 9:1025830.
doi: 10.3389/fmats.2022.1025830

An ultra-high performance concrete incorporating viscosity-controlling agent: Fiber distribution and microstructure

Baojun Zhao*, Zongjun Zhang, Chen Wu, Changgen Zou, Xin Xu, Han Yang and Wenqi Zhang

China State Construction Hailong Technology Co Ltd., Shenzhen, China

In order to realize the stability of steel fiber inside ultra-high performance Concrete (UHPC) under vibration and improve the use efficiency of fiber, bentonite is used as auxiliary cementitious material in this study. The influence of bentonite dosage on the mechanical properties of UHPC matrix and the mechanical properties and microstructure of ultra-high Performance fiber Reinforced Concrete (UHPFRC) is explored. On this basis, the functional relationships between the distribution and orientation of steel fibers, the freshness of the matrix and the rheological parameters of UHPC are established, and the evaluation model of the service efficiency of steel fibers is established. The results show that with the gradual increase of bentonite incorporation, the use efficiency of UHPFRC steel fiber increases first and then decreases, and when the cement content of bentonite was 2.5%, 5.0%, 7.5% and 10.0%, the flexural strength of UHPFRC increased by 9.0%, 17.6%, 18.5% and 6.1%, respectively. In addition, the increase of bentonite content will lead to the continuous decrease of the fluidity of fresh UHPC slurry (from 261 mm to 100 mm). When the bentonite content is 10.0%, the UHPC slurry has almost no fluidity (100 mm), which leads to the appearance of pores in the UHPC matrix and the decrease of compressive strength.

KEYWORDS

UHPC, UHPFRC, mechanical properties, rheological properties, the efficiency of fiber

1 Introduction

Ultra-high performance concrete (UHPC), as a new generation of cement-based building materials emerged in the 1990s, has superior mechanical properties, excellent toughness and excellent durability compared with ordinary concrete (Yu et al., 2015a; Yu et al., 2015b; Yunsheng et al., 2017). Fiber or polymer fiber is usually added to improve the mechanical properties of UHPC, especially steel fiber is added to bridge cracks and prevent crack propagation, so as to reduce the brittleness of mortar and improve mechanical strength and toughness (Song et al., 2018; Dingqiang et al., 2021; Zhang et al., 2022a; Zhang et al., 2022b; Zhang et al., 2022c). The UHPC reinforced concrete with fiber is called Ultra-high Performance Fiber Reinforced Concrete (UHPFRC). In recent

years, with the wide application of UHPC in the field of architecture, the performance research of UHPC and UHPFRC has attracted the attention of scholars around the world. Previous studies have shown that the addition of steel fibers can inhibit the generation and propagation of micro cracks and macro cracks (Wu et al., 2018; Huang et al., 2021), thereby improving the overall toughness of UHPFRC. In other words, steel fibers indeed have a significant impact on the mechanical properties of UHPC.

In most cases, fiber orientation and distribution in UHPFRC are random. Previous studies have shown that the optimized fiber orientation can increase the flexural strength and toughness by 60% and 80%, respectively (Meng and Khayat, 2017). However, the fiber effectiveness is only 30% due to the inhomogeneity of fiber orientation and the influence of flow and vibration parameters in the process of pouring and vibration in the preparation process. It has been reported that currently, the methods that can improve the fiber orientation and distribution of UHPFRC to improve the bending performance include controlling the rheological properties of UHPFRC matrix (Kang et al., 2011), selecting the casting method (Abrishambaf et al., 2017), and using electromagnetic fields in the casting process (Wang et al., 2017). However, although the excellent fluidity can ensure that the slurry can be cast and formed, it does not necessarily guarantee that the steel fiber can be uniformly suspended in the UHPC matrix. For example, Wang et al. (Conforti et al., 2017) found that the UHPC with high fluidity is difficult to resist the segregation and settlement of the steel fiber due to the lack of consolidation ability and weak shaping viscosity. The inhomogeneity of steel fiber is easy to introduce bubbles, which cannot guarantee the excellent mechanical properties of UHPFRC. Secondly, it is not enough to keep the excellent orientation and distribution of fiber in the pouring process. In the actual production process, the prepared UHPFRC samples are larger, and the fresh slurry needs to be compacted by vibration after pouring to remove bubbles. However, vibration may lead to the movement and rotation of fibers in some directions, and it is difficult to ensure the orientation and distribution of fibers in a relatively perfect state. Conforti et al. (Al-Shwaiter et al., 2021; Cai et al., 2021)believe that steel fibers tend to disordered orientation and settlement during vibration. At the same time, vibration will reduce the yield stress of "internal friction force" in the mixture and accelerate the settlement of steel fiber under gravity. Therefore, it is necessary to stabilize the steel fiber under vibration condition and improve the effectiveness of the fiber.

The way to improve the efficiency of fiber use is to use chemical admixture to adjust the rheological properties of fresh concrete, such as adding superplasticizer and viscosity modifier. Al-shwaiter and others (Kim et al., 2012) have improved the rheological properties with superplasticizer. However, the high cost of chemical admixture makes it not suitable for mass use in actual production. Therefore, scholars turned their attention from the introduction of admixture to the study of auxiliary cementitious materials, hoping to optimize the composition of concrete while improving the rheological properties. Bentonite is a low-cost, readily available 2:1 layered silicate clay mineral. It can absorb and discharge the water molecules between the unit layers, so as to adjust the rheological characteristics of fresh concrete, enhance the stability of steel fiber inside UHPFRC, improve the use efficiency of steel fiber, and improve its flexural strength. Kaci et al. (Yu et al., 2014) explored the influence of bentonite content on rheological properties, yield stress and viscosity of fresh cement paste. However, there is a lack of research on the application of bentonite in UHPC. At the same time, the use of bentonite to regulate the uniform distribution of steel fibers needs to be developed. Therefore, it is more important to study the influence of bentonite on the rheological properties of UHPFRC matrix and fiber orientation distribution on the mechanical properties.

In this paper, bentonite is used as the auxiliary cementitious material, and the influence mechanism of bentonite on the mechanical properties of UHPC and UHPFRC is obtained by studying and evaluating the influence of the amount of bentonite on the mechanical properties and microstructure of UHPC and UHPFRC. The synergistic effect of fiber orientation distribution and matrix rheological properties on the mechanical properties of UHPFRC is further analyzed, and the mechanism of steel fiber action on UHPFRC is obtained.

2 Materials and methods

2.1 Materials

UHPC uses ordinary Portland cement (52.5P O, OPC), silica fume (SF), lime powder (LP) and bentonite (BT) as cementing

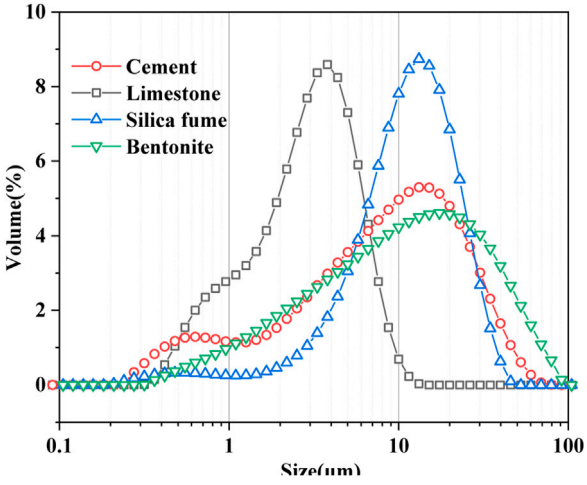

FIGURE 1
Particle size distributions of ingredients.

TABLE 1 Chemical composition of cementitious materials (wt%).

Composition	Al_2O_3	SiO_2	P_2O_5	SO_3	K_2O	Na_2O	MgO	CaO	Fe_2O_3	TiO_2
OPC	4.18	19.2	0.09	3.35	0.78	0.09	1.61	64.93	3.32	-
SF	0.25	94.65	0.17	0.69	0.84	0.13	0.47	0.36	0.15	-
LP	0.08	0.19	0.01	0.02	-	-	2.89	54.06	0.09	-
BT	15.60	64.25	0.21	-	3.86	2.80	2.50	1.63	4.60	0.60

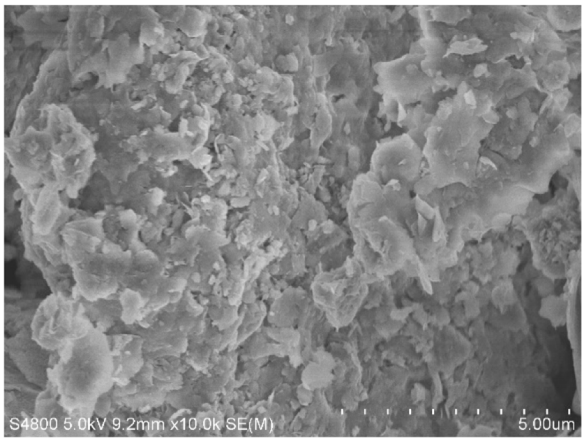

FIGURE 2
Appearance morphology of bentonite.

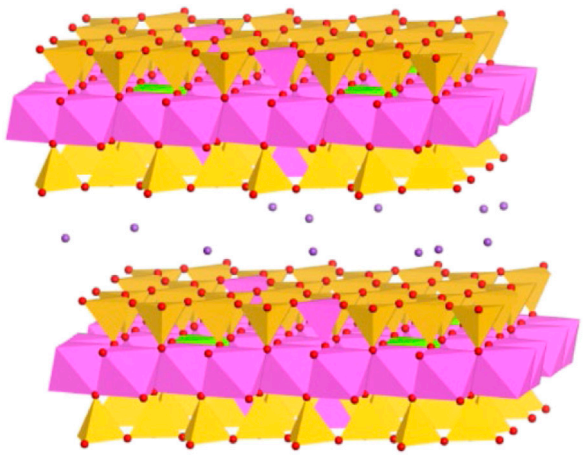

FIGURE 3
Crystal structures of montmorillonite.

materials, river sand (0–0.6 mm is fine sand, 0.6–1.25 mm is coarse sand) as fine aggregate and PC-10 polycarboxylic acid system superplasticizer (solid content 20%). The particle size distribution analysis of these powders is shown in Figure 1, and the chemical mixtures are listed in Table. 1. In addition, straight steel fibers with a length of 13 mm and a diameter of 0.2 mm are used.

Bentonite is a yellow-white flake clay with montmorillonite as the main component, and its microstructure is shown in Figure 2. Montmorillonite consists of two layers of silicon oxygen tetrahedra and one layer of aluminum oxide octahedron, which is a 2:1 layered silicate, as shown in Figure 3, its relative density is 2.4–2.8, and its specific surface area is 468.2 m^2/g. Al^{3+} and Si^{4+} in octahedral and tetrahedral structures can be replaced by low-cost cations to negatively charge the montmorillonite crystalline layer. The cations such as Na^+ and Ca^{2+} are adsorbed to the interlayer to balance the negative charge on the surface of montmorillonite. The structure characteristics of cation exchange in the montmorillonite lattice determine that the montmorillonite has good cation exchange, swelling, adsorption and thixotropy properties.

2.2. Design of mix ratio

On the basis of the existing literature (Yu et al., 2014), the improved Andreasen and Andersen model (A&A) is used to design the UHPC ratio. As shown in Table. 2, the dosage of bentonite instead of cement is 0.0%, 2.5%, 5.0%, 7.5% and 10.0%, respectively. The corresponding fresh slurry is prepared according to the experimental ratio. The mixing process of UHPC is shown in Figure 4. The fluidity of the prepared fresh slurry will be measured first, and the mechanical properties and microscopic morphology of the slurry will be tested after curing to the specified age after forming. For the preparation of UHPFRC, besides changing the dosage of bentonite, steel fiber with a volume fraction of 2% is added. At the same time, in order to explore the influence of fiber orientation and distribution on mechanical properties and rheological properties, the slurry is poured on one side of the mold after the slurry mixing is completed to optimize the orientation and distribution of steel fiber (Song et al., 2018). The mortar specimens are vibrated and compacted by shaking table for 120 s. After curing at room temperature for 24 h, the samples are removed from the film and placed in the steam curing environment for 48 h, and the corresponding strength is measured.

TABLE 2 Mix proportion of the UHPC/(kg/m^3).

Group	OPC	The dosage of BT (%)	BT	SF	LP	FS	CS	SP	W
0	750	0.0	0	150	200	770	220	35	190
1	731.25	2.5	18.75	150	200	770	220	35	190
2	712.5	5.0	37.5	150	200	770	220	35	190
3	693.75	7.5	56.25	150	200	770	220	35	190
4	675	10.0	75	150	200	770	220	35	190
5	656.25	12.5	93.75	150	200	770	220	35	190
6	637.5	15	112.5	150	200	770	220	35	190

(FS: fine sand; CS: coarse sand; SP: superplasticizer; W: Water).

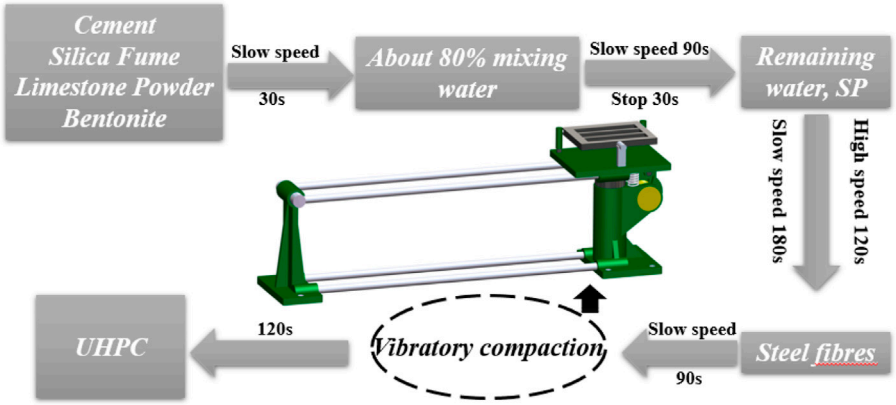

FIGURE 4
Mixing procedures of UHPC samples.

2.3 Test methods

2.3.1 Fluidity

In this experiment, the fluidity of UHPC is tested according to GB/T 2419-2005 named "Determination Method for Fluidity of cement mortar", in order to study the influence of bentonite incorporation on the workability of UHPC. Firstly, the stirred UHPC slurry is poured into the truncated cone round mold with the upper and lower hole diameters of 70 mm and 100 mm, respectively, and the height of 60 mm. The excess slurry is scraped off until it is flush with the upper surface of the mold. Then lift the mold vertically at a slow and uniform speed to allow the slurry to flow out completely. After the flow of UHPC slurry stops, measure the longest diameter and its vertical diameter and take the average of the two as the fluidity.

2.3.2 Rheological property

Rheological properties (Plastic viscosity, Yield stress and Thixotropy) are characterized by shear-rate-controlled protocol. The rheological properties for the fresh UHPC slurry were tested using a rotor type viscometer (Brookfield Company, R/S-SST, 20 × 10 mm rotor). The test rheological program for UHPC using shear rate control is presented in Figure 5. First, the fresh UHPC slurry was measured for 30 s at a constant shear rate of 25 s^{-1}. Next, the slurry should be rested for 60 s. At last, the fresh UHPC slurry was tested under a different shear rate growth and decline protocol for 60 s, and this rate was changed from 0 to 25 s^{-1} to 0.

Fresh UHPC slurry is a multiphase fluid, which is generally characterized by complex non-Newtonian fluid. Generally, Herschel-Bulkley model (H-B) (Yu et al., 2021) which can more accurately characterize the dynamic yield stress and consistency coefficient (K) of UHPC is employed to characterize the dynamic yield stress of the cement, mortar or concrete pastes based on fitting lines of the flow curves. Shear stress (τ) and the shear rate ($\dot{\gamma}$) are used to evaluate, expressed by Eq. 1:

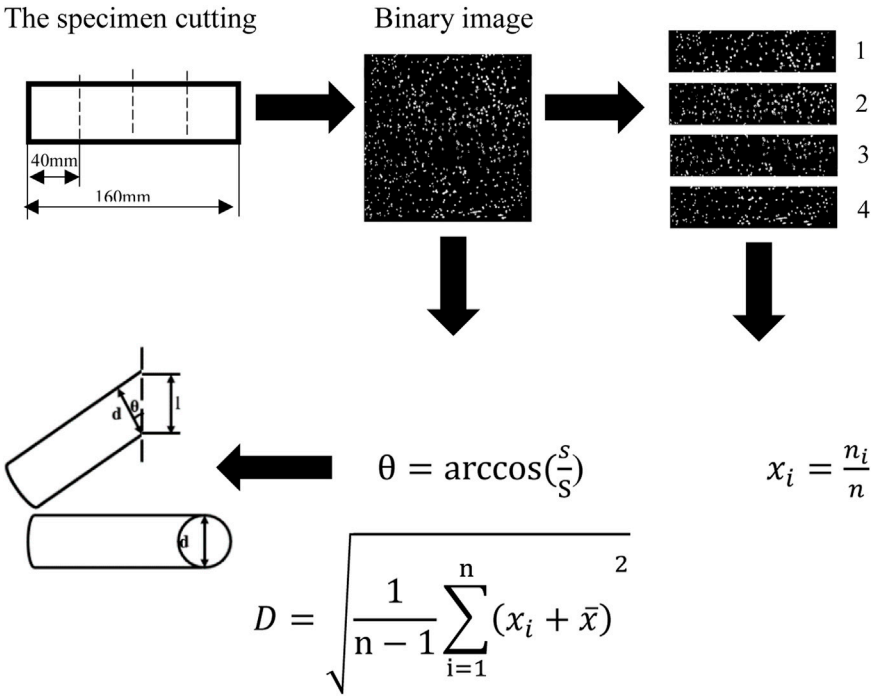

FIGURE 5
Image processing procedures.

Herschel-Bulkley (H-B) model:

$$\tau = \tau_0 + \omega\dot{\gamma}^n\mu = \frac{3\omega}{n+2}\dot{\gamma}_{max}^{n-1}, \quad (1)$$

where τ is shear stress (Pa); τ_0 yield stress (Pa); μ is plastic viscosity (Pas); $\dot{\gamma}$ is shear rate (s^{-1}); ω is consistency coefficient (Pas^n), in which n = 1; n > 1for shear thickening, dilatant fluid; n < 1, for shear thinning, pseudoplastic fluid.

For a dynamic shear rate, the change in the thixotropy is attributed to the attenuation of shear stress from up value to down value (Chen et al., 2020). The fully enclosed thixotropic loop calculated from the data can characterize the collapse of the slurry structure. Its area is calculated by Eq. 2:

$$A = \int_{\dot{\gamma}min}^{\dot{\gamma}max} \eta_1\dot{\gamma}d\dot{\gamma} - \int_{\dot{\gamma}min}^{\dot{\gamma}max} \eta_2\dot{\gamma}d\dot{\gamma}, \quad (2)$$

where A represents the area of thixotropic loop; η_1 represents high apparent viscosity (Pas); η_2 represents low apparent viscosity (Pas); $\dot{\gamma}$ represents shear rate (s^{-1}).

2.3.3 Mechanical properties

This experiment is based on GB/T 17,671-1999 named "cement mortar strength test Method (ISO method)" as the standard, to test the mechanical properties of UHPC. After 48 h steam curing (curing conditions, temperature and humidity), the flexural strength and compressive strength of UHPC test block are tested. Each mixture is tested three times in duplicate, and then the average value is taken as the result. The mechanical property test instrument used is the pressure testing machine (JES-2000A) produced by Wuxi Xidong Building Materials Equipment Factory.

2.3.4 Analysis of steel fiber orientation and distribution

For the evaluation of fibre orientation and distribution, the specimens are cut into three slices parallel to the casting direction that are numbered from A1 to A3, the cross section was converted into binary image (Song et al., 2018) and then divided into four equal pieces that are numbered from 1 to 4 with the position from the casting surface to the bottom of specimen, and the area proportion and number of the steel fibres per unit are counted as shown in Figure 5.

When the fibers in UHPC tend to be lengthwise, the average angle of fibers in the cross section of the specimen is the smallest. The fiber orientation in UHPC can be expressed by the average angle of the fiber, that is, the smaller the average fiber angle, the better the fiber orientation. It can also be expressed that when the fiber area in the cross section is smaller, the orientation of the fiber is better. When the fibers in the UHPC are completely uniformly distributed, the number of fibers at each position in the cross section of the sample is the same, that is, the percentage of fibers at each position is the same. Therefore, the variance of fiber

number percentage can be used to characterize the uniformity of fiber distribution in the sample, that is, the smaller the variance, the more uniform the fiber distribution in the sample.

The angle (θ) between the fibre axis and the normal direction is used to quantitatively assess the steel fibre orientation across the cross section according to Eq. 3 (Teng et al., 2020).

$$\theta = \arccos\left(\frac{d}{l}\right) = \arccos\left(\frac{\pi d^2/4}{\pi dl/4}\right) = \arccos\left(\frac{s}{S}\right), \quad (3)$$

where d and s are the diameter and the area of the steel fibre, respectively; l and S are the major axis and the average area of the steel fibre image, respectively.

The variance of the steel fibre counts percentage ($\boldsymbol{D}$) was used to represent steel fibres distribution by Eq. Eq. 4 and Eq. 5 (Song et al., 2018):

$$x_i = \frac{n_i}{n}, \quad (4)$$

$$D = \sqrt{\frac{1}{\mathrm{n}-1}\sum_{\mathrm{i}=1}^{\mathrm{n}}(x_i + \bar{x})^2}, \quad (5)$$

Where x_i is the percentage of the number of steel fibres; n is the number of steel fibres on the cross section. ni is the number of steel fibres in piece image i; $\bar{x}$ is the average number of steel fibres in all four pieces.

2.3.5 Microstructure

In this study, field emission scanning electron microscopy (SEM) of QUANTA FEG450 is used to characterize the microstructure of UHPC after steaming. After curing treatment, the UHPC sample is cut into small pieces and soaked in ethanol to prevent hydration. All samples are then dried in a vacuum at 80 ± 2°c for 6 h and then sprayed with platinum for testing.

3 Results and discussions

3.1 Fluidity

The results of fluidity of UHPC with different bentonite doping contents are shown in Figure 6. As can be seen from the figure, with the incorporation of bentonite, the fluidity of freshly mixed UHPC slurry decreases continuously. In this experiment, the UHPC slurry without bentonite (standard group) has the highest mobility of 261 mm. After adding 2.5%, 5.0% and 7.5% bentonite, the fluidity decreased by 10.3%, 32.0% and 54.0%, respectively, compared with the standard group. When the bentonite content is 10.0%, the freshly mixed UHPC slurry has almost no fluidity, and the viscosity of the slurry is high with a fluidity of 100 mm. The above phenomena can be explained by the mechanism of bentonite action. On the one hand, bentonite has a large specific surface area and layered

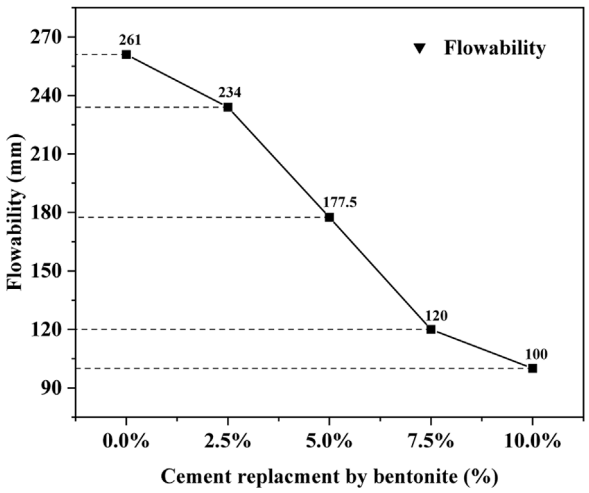

FIGURE 6
Flowability of the designed UHPC.

microstructure, and its surface energy is usually reduced by adsorption of water molecules, which leads to a decrease in the free water of dispersed cement (Kaci et al., 2011; Xie et al., 2018), therefore, the fluidity of freshly mixed UHPC slurry decreases. On the other hand, bentonite can adsorb superplasticizer on the surface because of its special structure (Ng and Plank, 2012). For example, Wang Hao et al. (Hao et al., 2016) studied the influence and mechanism of Na-based montmorillonite on the fluidity of cement, and the results showed that when the cement substitution mass fraction of Na-based montmorillonite was 3%, its adsorption capacity for superplasticizer was 2.16 times of that of cement material, which was 18.33 mg/g. Therefore, the larger the bentonite content is, the more obvious the adsorption effect of superplasticizer is, leading to the inhibition of free water dispersion and the decrease of slurry fluidity.

3.2 Mechanical properties of UHPC

The influence of bentonite on the mechanical properties of UHPC matrix is studied. The relationship between different bentonite doping content and the development of compressive strength and flexural strength of UHPC is shown in Figure 7. As can be seen from the figure, when the bentonite content increases from 0% to 5.0%, the compressive strength of UHPC matrix is about 120 MPa. When the content of bentonite increases to 7.5% and 10.0%, the strength decreases slightly, but still exceeds 100 MPa. In addition, it can be seen that the flexural strength of UHPC matrix is about 13–14 MPa, which does not change significantly with the addition of bentonite.

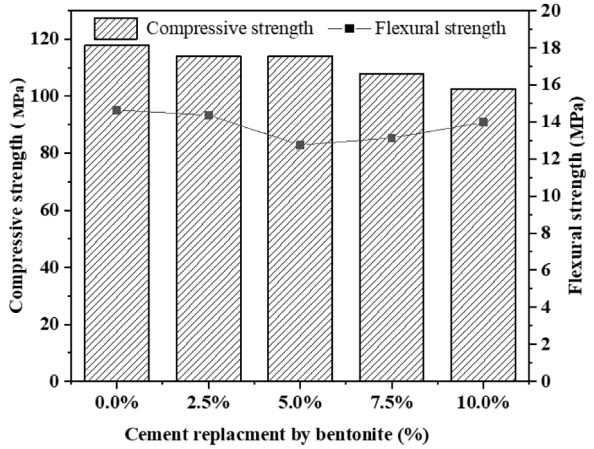

FIGURE 7
Compressive strength and flexural strength of UHPC matrix.

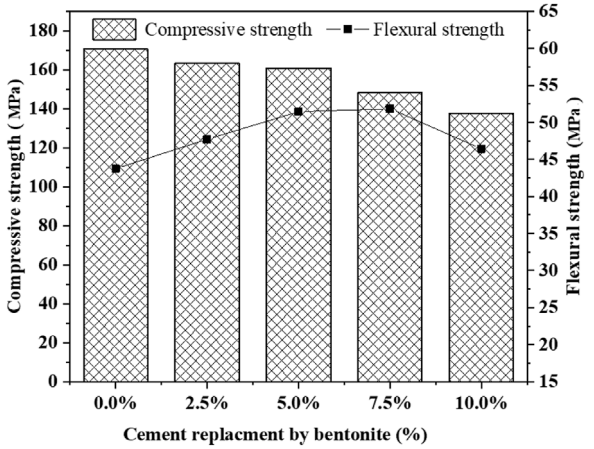

FIGURE 8
Compressive strength and flexural strength of UHPFRC.

There are two main reasons for the decrease of the compressive strength mentioned above: 1) the microstructure of the matrix is loose and porous due to the high bentonite content (Xie et al., 2019), so the strength of the matrix is easy to decrease due to the high bentonite content; 2) At the same time, the increase of bentonite incorporation also leads to the decrease of fluidity and the increase of the viscosity of the matrix, so that a large amount of air is trapped in the matrix (Teng et al., 2020), which further leads to the decrease of strength. However, when the content of bentonite is within a certain range, bentonite can be used as a reliable auxiliary cementing material to maintain the excellent mechanical properties of concrete products. Therefore, bentonite as a viscosity regulator can optimize the viscosity within a certain dosage range without damaging the development of strength.

3.3 Mechanical properties of UHPFRC

To further study the effect of bentonite on the mechanical properties of UHPFRC. The relationship between different bentonite doping content and the development of compressive strength and flexural strength of UHPFRC is shown in Figure 8. It can be seen that the compressive strength of UHPFRC is 170 MPa when no bentonite is added. When the bentonite content is 2.5% and 5.0%, the compressive strength of UHPFRC is about 160 MPa. But the compressive strength of UHPFRC decreases significantly by 13.1% and 19.3% compared with the standard group, respectively, when he bentonite increased to 7.5% and 10.0%. This is because when the content of bentonite is too much, the flow of UHPC slurry is too low, which leads to the agglomeration of steel fibers. When the steel fibers are too concentrated, the fiber orientation will be disorderly and the pores in the matrix will be dense. At the same time, the concentrated steel fibers may become stress concentration points, which will bring adverse effects on the strength.

In addition, it can be seen from Figure 8 that the flexural strength of UHPFRC is only 43.8 MPa without bentonite. With the increasing of bentonite content, the flexural strength of UHPFRC increased by 9.0%, 17.6%, 18.5%, and 6.1%, respectively, corresponding to 47.7 MPa, 51.5 MPa, 51.9 MPa and 46.5 MPa. This is because after adding bentonite, the fluidity of UHPC slurry is reduced and the cohesion of UHPC slurry is increased. As a result, the steel fiber with the vibrations of slurry in the bonding state still can maintain a good stability, which can provide greater crack bridging capacity and helps to significantly improve the flexural strength of UHPFRC, but the optimization of compressive strength is not obvious. In order to further analyze the reasons for the influence of bentonite content on the mechanical properties of UHPFRC, the use efficiency, orientation and distribution of steel fibers are studied in the following sections.

3.4 Use efficiency of steel fiber

Fiber service efficiency (E_f) is used to evaluate the effectiveness of steel fibers in UHPFRC. The calculation formula of steel fiber efficiency is shown in Eq. 6 (Gong et al., 2022; Ravichandran et al., 2022).

$$E_f = \frac{(f_i - f_0)}{n}. \quad (6)$$

E_f represents the efficiency of steel fiber. f_i represents the flexural strength of UHPFRC prepared with different bentonite content. f_0 represents the flexure strength of UHPC prepared

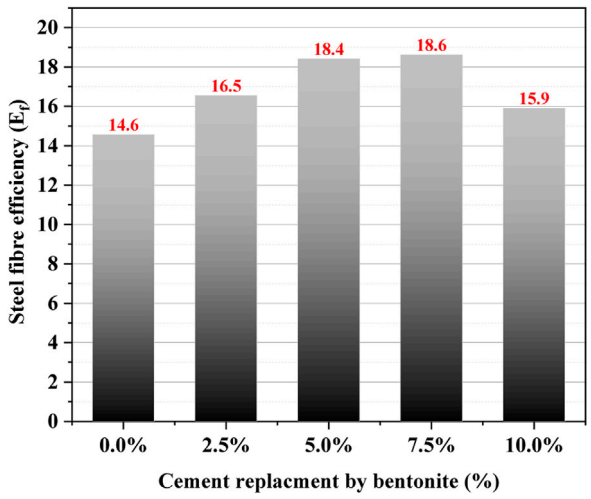

FIGURE 9
Steel fiber efficiency of UHPFRC.

without bentonite and steel fibers. N represents the volume content of steel fiber.

The use efficiency of steel fibers of UHPFRC prepared with different bentonite doping contents is shown in Figure 9. It can be seen that with the increase of bentonite content, the UHPFRC steel fiber use efficiency first increases to the maximum value and then decreases, which is still higher than the UHPFRC steel fiber use efficiency without bentonite. As we all know, the use efficiency of steel fiber is closely related to the orientation and distribution of steel fiber. When the orientation and distribution of steel fiber in UHPFRC are in a good state, the toughness of UHPFRC and the effectiveness of steel fiber are higher. Therefore, the above phenomenon can be attributed to the fact that the addition of bentonite is beneficial to the good orientation and distribution and stability of steel fibers, especially the high bond with the concrete matrix under vibration condition. However, when the amount of bentonite is too large, the workability of UHPC slurry is poor, and the negative effect of bentonite on steel fiber is greater than the positive effect, and the effectiveness of steel fiber decreases.

3.5 Steel fiber orientation and distribution

The binary image of the UHPC cutting plane is shown in Figure 10, from which the steel fiber information on the section can be obtained, including the number and distribution of steel fibers. The replacement of cement with bentonite can improve the distribution of steel fibers, as shown in Figure 10C,D,E.

The distribution of steel fibers is quantified by the percentage of steel fibers counted (*D*). When the bentonite dosage increases from 0.0% to 10.0%, *D* gradually decreases to the minimum, and then increases with the further increase of bentonite dosage. It should be noted that the *D* value on the cross section of UHPC with bentonite is always smaller than that of UHPC without bentonite, which means that the distribution of steel fibers in UHPC with bentonite tends to be uniform. The lower the *D* value, the more uniform the distribution of steel fibers. When the content of bentonite is 10%, *D* value is the smallest. This may be related to the addition of bentonite, which regulates the rheological properties of the slurry and makes the distribution of steel fibers more uniform.

The variation of UHPC steel fiber content along the casting depth is shown in Figure 11. 1–4 indicates the position of the sample from the surface to the bottom. The results show that when the steel fiber volume is 2%, the content of steel fiber in UHPC with different bentonite content fluctuates irregularly with the change of depth. When bentonite is not added, the number of steel fibers at the bottom is large, indicating that the dispersion of steel fibers in the sample is poor. This may partly be attributed to the higher fluidity, which does not guarantee the suspension of steel fibers in the UHPC matrix (Teng et al., 2020). The above phenomena correspond to the change trend of the bending strength of steel fiber UHPC.

3.6 Effect of steel fiber orientation distribution on flexural strength

As a kind of fiber reinforced composite material, the bending and cracking resistance of UHPC are closely related to the variation of fiber length and volume (Yoo et al., 2016; Yoo et al., 2017; Zhang et al., 2022d; Wen et al., 2022; Yoo et al., 2022; Zheng et al., 2022), the interfacial properties between fiber and matrix (Shannag et al., 1997; Wu et al., 2018; Mo et al., 2021), and the fiber distribution and orientation (Zerbino et al., 2012; Huang et al., 2018; Meng et al., 2022). When the orientation of the steel fiber is parallel to the direction of the main tensile stress, the effectiveness of the fiber in the bridge crack is the highest. For randomly oriented fibers, the effective rate is reduced to 30% (Azevedo et al., 2022). Excessive fiber incorporation will lead to uneven accumulation and distribution of UHPC, so the bending resistance of UHPC matrix is reduced (Kang and Kim, 2011). Therefore, when the fiber is uniform, the orientation corresponding to the principal tensile stress is improved, which can bridge cracks and resist cracks more effectively.

Figure 12 shows the relationship between different orientations and distributions of steel fibers in UHPC and compressive strength. It can be seen from Figure 12A that the bending strength of UHPC is the highest when the orientation *S* value of steel fiber is between 0.2 and 0.26. However, the change of adjacent *S* values in the figure leads to excessive changes in the increase and decrease amplitude. This is because all the UHPC samples in this experiment are poured on one side, and their orientations are uniform and within the optimized range, which

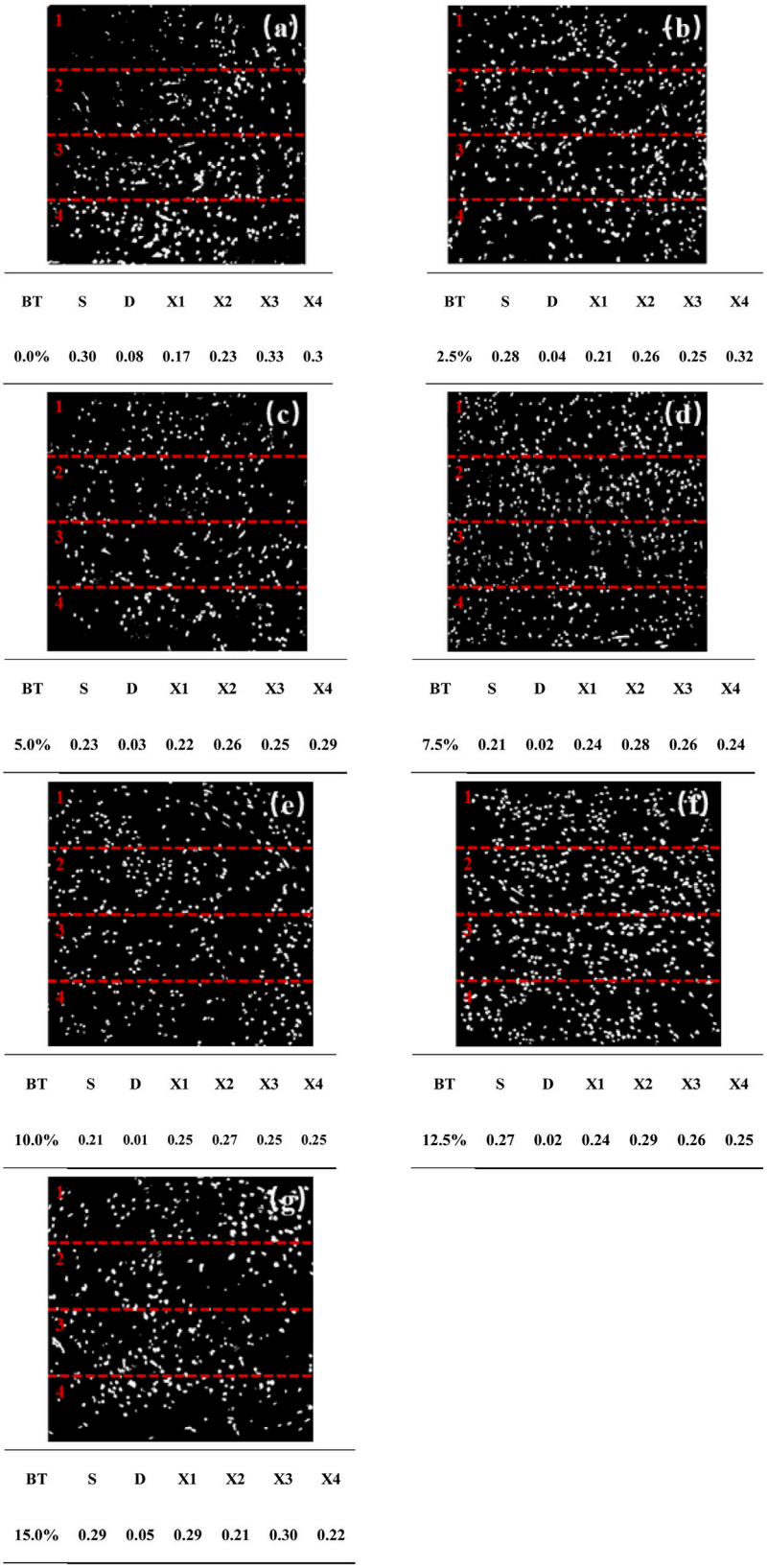

FIGURE 10
Binary images of steel fibres of the UHPC with different content of bentonite **(A)** 0%, **(B)** 2.5%, **(C)** 5%, **(D)** 7.5%, **(E)** 10%, **(F)** 12.5%, **(G)** 15%.

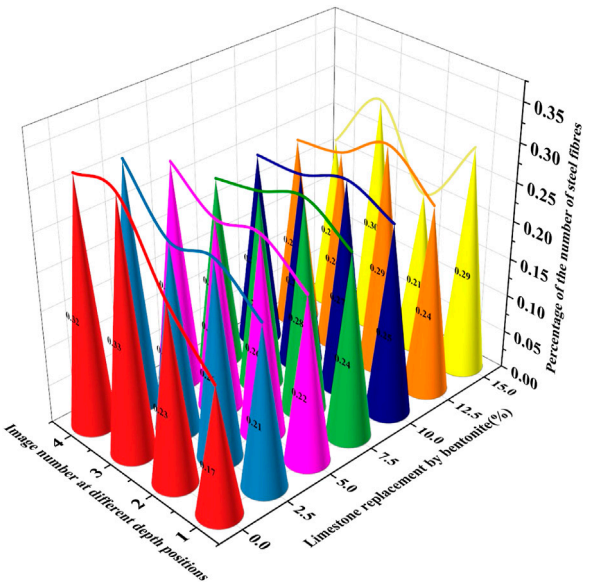

FIGURE 11
Variation of steel fibre content on different depth positions.

had certain limitations in influencing the flexion strength. As can be seen from Figure 12B, when the distribution of steel fibers is gradually uniform, the flexural strength of UHPC gradually increases. In addition, when the bentonite content is 15%, the ***D*** value is 0.046, but the flexural strength is higher than that of 2.5% and 5.0% UHPC (***D*** value is 0.043 and 0.034). This is because when the bentonite content is 15.0%, UHPC has higher the plastic viscosity and stronger binding force at the interface between the steel fiber and the matrix of UHPC is increased, which results in higher flexural strength. Therefore, when the steel fiber orientation is within the optimized range, the fiber distribution can improve the effectiveness of the fiber in the bridging crack, so as to improve the flexural performance and flexural strength of UHPC.

3.7 Correlation on of fibre orientation, distribution and rheological parameters

The state of fibre orientation and distribution in specimen actually results from adding bentonite as a rheology modifier, which is related to rheological performance of fresh UHPC slurry. The correlation between rheological performance and fibre orientation and distribution of UHPC is presented in Figure 13. All these parameters have a strong correlation and influence with each other. With the rise of yield stress, plastic viscosity, flowability and area of thixotropic loop, the steel fibre counts percentage (***D***) and the average area of the steel fibre image(***S***) of steel fibres decrease gradually at initial stage, and then increase after reaching the minimum value. The above phenomenon can be attributed to two aspects: 1) the sufficiently high yield stress, plastic viscosity and thixotropy are required to provide high resistance to steel fibre settlement during the vibration compaction process (Yoo et al., 2016); 2) the excessive yield stress, plastic viscosity and thixotropy may provide negative effects on the steel fibre orientation and distribution during the mixing process (Wang et al., 2017).

Based on the polynomial model and the extreme model (Eq. 8 and (9)), the average of ***D*** and the average of ***S*** occurred a

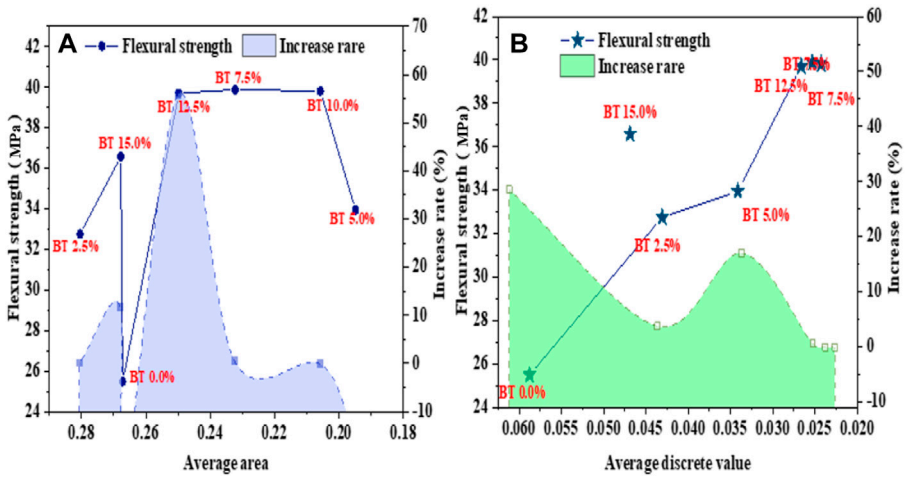

FIGURE 12
Change of flexural strength with orientation and distribution of steel fiber: **(A)** is orientation *S*, **(B)** is distribution *D*.

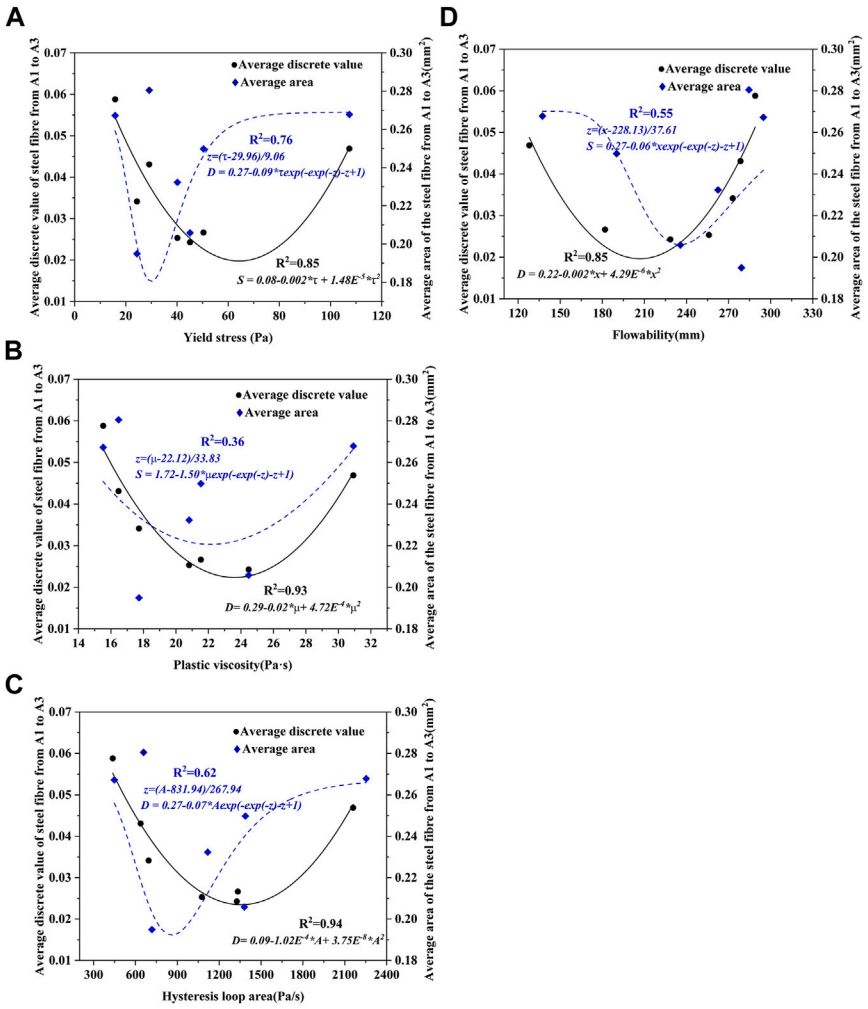

FIGURE 13
The evolution of *D* and *S* with **(A)** yield stress; **(B)** plastic viscosity; **(C)** area of thixotropic loop; **(D)** flowability under different bentonite content.

correlation with the variation of rheological parameters for these seven bentonite contents, respectively (Ozyurt et al., 2007).

The polynomial model:

$$D = I + a^{*}R + b^{*}x^{2}. \tag{7}$$

The extreme model:

$$\begin{cases} z = \dfrac{(R - R_c)}{c}, \\ S = S_0 + d^{*}\exp(-z) - z + 1, \end{cases} \tag{8}$$

Where R is the rheological parameters; a, b, c, d, I, z is a constant.

The ***S*** and the ***D*** are respectively plotted against rheological parameters and the best fitted curves are obtained from the data plots, as shown in Figure 13A–D. Firstly, there exists a correlation between ***D*** and yield stress, plastic viscosity, thixotropy, and flowability, with good correlation coefficients of 0.85, 0.93, 0.94 and 0.85, respectively. Which means that ***D*** has a strong correlation with rheological properties, and the influence of ***D*** on rheology is mainly governed by plastic viscosity and thixotropy. Therefore, more accurate steel fibre distribution can be reflected by plastic viscosity and thixotropy. Secondly, the correlations between ***S*** and yield stress, plastic viscosity, thixotropy and viscosity have certain limitations, and the correlation coefficients are 0.76, 0.36, 0.62, and 0.55, respectively. This means that the fibre orientation is mainly dominated by the rheological yield stress.

In summary, fibre distribution is more significantly affected by rheological changes than fibre orientation. At the same time, it shows that the steel fibres distribution is mainly governed by the plastic viscosity and thixotropy, while the steel fibre orientation is mainly dominated by the yield stress. Based on fibre distribution and orientation result, the ***D*** and ***S*** of UHPC ranges among 0.112–0.032, 0.200–0.279 respectively for UHPC with 5%, 10.0% and 12.5% bentonite. This indicates that the steel fibre

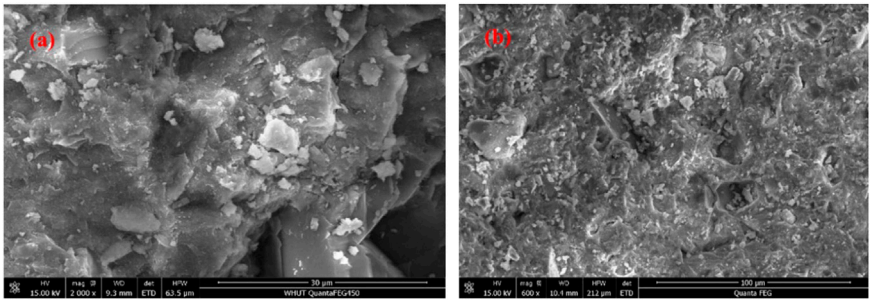

FIGURE 14
Microstructure of UHPC the dosage of BT=10%, **(A)** the surface of BT, **(B)** the microstructure of matrix.

distribution and orientation in UHPC are optimized, which can improve the homogeneity in the matrix and reduce macroscopic defects, thereby increasing the mechanical strength. This is consistent with the improvement of UHPC flexural strength. In addition to the change of fiber arrangement caused by the effect of bentonite on rheological properties, the effect of bentonite on matrix morphology is also explored later.

3.8 Microstructure of UHPC matrix

The microstructure of UHPC without and with bentonite are shown in Figure 14A and Figure 14B, respectively. It can be seen from the figure that the matrix structure of UHPC without bentonite is smooth and compact, which is the source of the excellent mechanical properties of UHPC. Although the morphology of bentonite is also dense, there are still some pores. This is because when the content of bentonite is too high, the fluidity of UHPC slurry is low, and a large number of bubbles brought in during the stirring process cannot be discharged during the vibration compaction process, thus forming pores. This is also the reason why the compressive strength of UHPC matrix decreases when the content of bentonite increases to 10.0%.

4 Conclusion

1) With the incorporation of bentonite, the fluidity of freshly mixed UHPC slurry showes a downward trend. When the incorporation amount of bentonite is 10.0%, the fresh UHPC slurry has almost no fluidity, and the slurry has high cohesion.
2) When the bentonite content is less than 5.0%, the compressive strength of UHPC matrix is about 120MPa; With the increase of bentonite content, the flexural strength of UHPC matrix does not change much and remains in the range of 13–14 MPa. The flexural strength of UHPFRC increase by 9.0%, 17.6%, 18.5% and 6.1%, respectively, with the gradual increase of bentonite content. In addition, when the bentonite content is 2.5% and 5.0%, compared with the non-bentonite UHPFRC whose compressive strength is about 170 MPa, the compressive strength only decreases by about 10 MPa–160 MPa, which still has excellent mechanical properties.
3) The functional correlation between the steel fibres distribution and orientation and the rheological parameters of fresh UHPC is established. The obtained results show that based on an optimized rheology control, the fibre orientation and distribution in UHPC can be well optimized in this study. It is particularly noteworthy that the variation of rheological parameters more significant effect on distribution than orientation of steel fibres. To be specific, the fibre distribution is mainly governed by the plastic viscosity and thixotropy, while the fibre orientation is mainly dominated by the yield stress.
4) The use-efficiency model of steel fiber shows that the use-efficiency of UHPFRC mixed with bentonite is always higher than that of UHPFRC not mixed with bentonite. In addition, with the increase of bentonite content, the use efficiency of UHPFRC steel fiber showes a trend of first increasing and then decreasing.

Data availability statement

The original contributions presented in the study are included in the article/supplementary material, further inquiries can be directed to the corresponding author.

Author contributions

BZ, ZZ, CW, CZ, XX designed research, performed research, analyzed data, and wrote the paper.

Conflict of interest

BZ, ZZ, CW, CZ, XX, HY, and WZ were employed by China State Construction Hailong Technology Co Ltd.

Publisher's note

References

Abrishambaf, A., Pimentel, M., and Nunes, S. (2017). Influence of fibre orientation on the tensile behaviour of ultra-high performance fibre reinforced cementitious composites. *Cem. Concr. Res.* 97, 28–40. doi:10.1016/j.cemconres.2017.03.007

Al-Shwaiter, A., Awang, H., and Khalaf, M. A. (2021). The influence of superplasticiser on mechanical, transport and microstructure properties of foam concrete. *J. King Saud Univ.* doi:10.1016/j.jksues.2021.02.010

Azevedo, A. R. G., Lima, T. E. S., Reis, R. H. M., Oliveira, M. S., Candido, V. S., and Monteiro, S. N. (2022). Guaruman fiber: A promising reinforcement for cement-based mortars. *Case Stud. Constr. Mater.* 16, e01029. doi:10.1016/j.cscm.2022.e01029

Cai, Y., Liu, Q.-F., Yu, L., Meng, Z., Hu, Z., Yuan, Q., et al. (2021). An experimental and numerical investigation of coarse aggregate settlement in fresh concrete under vibration. *Cem. Concr. Compos.* 122, 104153. doi:10.1016/j.cemconcomp.2021.104153

Chen, M., Yang, L., Zheng, Y., Huang, Y., Li, L., Zhao, P., et al. (2020). Yield stress and thixotropy control of 3D-printed calcium sulfoaluminate cement composites with metakaolin related to structural build-up. *Constr. Build. Mater.* 252, 119090. doi:10.1016/j.conbuildmat.2020.119090

Conforti, A., Plizzari, G., and Zerbino, R. (2017). Vibrated and self-compacting fibre reinforced concrete: Experimental investigation on the fibre orientation. *IOP Conf. Ser. Mat. Sci. Eng.* 246, 012019. doi:10.1088/1757-899x/246/1/012019

Dingqiang, F., Yu, R., Kangning, L., Junhui, T., Zhonghe, S., Chunfeng, W., et al. (2021). Optimized design of steel fibres reinforced ultra-high performance concrete (UHPC) composites: Towards to dense structure and efficient fibre application. *Constr. Build. Mater.* 273, 121698. doi:10.1016/j.conbuildmat.2020.121698

Gong, J., Ma, Y., Fu, J., Ouyang, X, Xhang, Z, Wang, H, et al. (2022). Utilization of fibers in ultra-high performance concrete: A review[J]. *Compos. Part B Eng.* 241, 109995. doi:10.1016/j.compositesb.2022.109995

Hao, W., Shujun, G., and Aifeng, Z. (2016). Study on mechanism of fluidity deterioration of fresh cement by sodium montmorillonite. *China Build. Mater.* 2016, 130–133. doi:10.16291/j.cnki.zgjc.2016.05.035

Huang, H., Gao, X., Li, L., and Wang, H. (2018). Improvement effect of steel fiber orientation control on mechanical performance of UHPC. *CONSTR BUILD MATER* 188, 709–721. doi:10.1016/j.conbuildmat.2018.08.146

Huang, H., Gao, X., and Khayat, K. H. (2021). Contribution of fiber alignment on flexural properties of UHPC and prediction using the Composite Theory. *Cem. Concr. Compos.* 118, 103971. doi:10.1016/j.cemconcomp.2021.103971

Kaci, A., Chaouche, M., and Andréani, P. A. (2011). Influence of bentonite clay on the rheological behaviour of fresh mortars. *Cem. Concr. Res.* 41, 373–379. doi:10.1016/j.cemconres.2011.01.002

Kang, S., and Kim, J. (2011). The relation between fiber orientation and tensile behavior in an ultra high performance fiber reinforced cementitious composites (UHPFRCC). *Cem. Concr. Res.* 41 (10), 1001–1014. doi:10.1016/j.cemconres.2011.05.009

Kang, S. T., Lee, B. Y., Kim, J.-K., and Kim, Y. Y. (2011). The effect of fibre distribution characteristics on the flexural strength of steel fibre-reinforced ultra high strength concrete. *Constr. Build. Mater.* 25, 2450–2457. doi:10.1016/j.conbuildmat.2010.11.057

Kim, H. K., Jeon, J., and Lee, H. (2012). Workability, and mechanical, acoustic and thermal properties of lightweight aggregate concrete with a high volume of entrained air. *Constr. Build. Mat.* 29, 193–200. doi:10.1016/j.conbuildmat.2011.08.067

Meng, S., Jiao, C., Ouyang, X., Niu, Y., and Fu, J. (2022). Effect of steel fiber-volume fraction and distribution on flexural behavior of Ultra-high performance fiber reinforced concrete by digital image correlation technique. *CONSTR BUILD MATER* 320, 126281. doi:10.1016/j.conbuildmat.2021.126281

Meng, W., and Khayat, K. H. (2017). Improving flexural performance of ultra-high-performance concrete by rheology control of suspending mortar. *Compos. Part B Eng.* 117, 26–34. doi:10.1016/j.compositesb.2017.02.019

Mo, Z., Gao, X., and Su, A. (2021). Mechanical performances and microstructures of metakaolin contained UHPC matrix under steam curing conditions. *Constr. Build. MATER* 268, 121112.

Ng, S., and Plank, J. (2012). Interaction mechanisms between Na montmorillonite clay and MPEG-based polycarboxylate superplasticizers. *Cem. Concr. Res.* 42, 847–854. doi:10.1016/j.cemconres.2012.03.005

Ozyurt, N., Mason, T. O., and Shah, S. P. (2007). Correlation of fiber dispersion, rheology and mechanical performance of FRCs. *Cem. Concr. Compos.* 29, 70–79. doi:10.1016/j.cemconcomp.2006.08.006

Ravichandran, D., Prem, P. R., Kaliyavaradhan, S. K., and Ambily, P. (2022). Influence of fibers on fresh and hardened properties of ultra high performance concrete (UHPC)—a review. *J. Build. Eng.* 57, 104922. doi:10.1016/j.jobe.2022.104922

Shannag, M. J., Brincker, R., and Hansen, W. (1997). Pullout behavior of steel fibers from cement-based composites. *Cem. Concr. Res.* 27 (6), 925–936. doi:10.1016/s0008-8846(97)00061-6

Song, Q., Yu, R., Shui, Z., Wang, X., Rao, S., and Lin, Z. (2018). Optimization of fibre orientation and distribution for a sustainable ultra-high performance fibre reinforced concrete (UHPFRC): Experiments and mechanism analysis. *Constr. Build. Mater.* 169, 8–19. doi:10.1016/j.conbuildmat.2018.02.130

Teng, L., Meng, W., and Khayat, K. H. (2020). Rheology control of ultra-high-performance concrete made with different fiber contents. *Cem. Concr. Res.* 138, 106222. doi:10.1016/j.cemconres.2020.106222

Wang, R., Gao, X., Huang, H., and Han, G. (2017). Influence of rheological properties of cement mortar on steel fiber distribution in UHPC. *Constr. Build. Mater.* 144, 65–73. doi:10.1016/j.conbuildmat.2017.03.173

Wen, C., Zhang, P., Wang, J., and Hu, S. (2022). Influence of fibers on the mechanical properties and durability of ultra-high-performance concrete: A review. *J. Build. Eng.* 52, 104370. doi:10.1016/j.jobe.2022.104370

Wu, Z., Khayat, K. H., and Shi, C. (2018). How do fiber shape and matrix composition affect fiber pullout behavior and flexural properties of UHPC? *Cem. Concr. Compos.* 90, 193–201. doi:10.1016/j.cemconcomp.2018.03.021

Xie, Y., Li, J., Lu, Z., Jiang, J., and Niu, Y. (2018). Effects of bentonite slurry on air-void structure and properties of foamed concrete. *Constr. Build. Mater.* 179, 207–219. doi:10.1016/j.conbuildmat.2018.05.226

Xie, Y., Li, J., Lu, Z., Jiang, J., and Niu, Y. (2019). Preparation and properties of ultra-lightweight EPS concrete based on pre-saturated bentonite. *Constr. Build. Mater.* 195, 505–514. doi:10.1016/j.conbuildmat.2018.11.091

Yoo, D., Jang, Y. S., Oh, T., and Banthia, N. (2022). Use of engineered steel fibers as reinforcements in ultra-high-performance concrete considering corrosion effect. *Cem. Concr. Compos.* 133, 104692. doi:10.1016/j.cemconcomp.2022.104692

Yoo, D., Kang, S., and Yoon, Y. (2016). Enhancing the flexural performance of ultra-high-performance concrete using long steel fibers. *COMPOS Struct.* 147, 220–230. doi:10.1016/j.compstruct.2016.03.032

Yoo, D., Kim, S., Park, G., Park, J., and Kim, S. (2017). Effects of fiber shape, aspect ratio, and volume fraction on flexural behavior of ultra-high-performance fiber-reinforced cement composites. *COMPOS Struct.* 174, 375–388. doi:10.1016/j.compstruct.2017.04.069

Yu, R., Spiesz, P., and Brouwers, H. J. H. (2015). Development of ultra-high performance fibre reinforced concrete (UHPFRC): Towards an efficient utilization of binders and fibres. *Constr. Build. Mater.* 79, 273–282. doi:10.1016/j.conbuildmat.2015.01.050

Yu, R., Spiesz, P., and Brouwers, H. J. H. (2015). Development of an eco-friendly Ultra-High Performance Concrete (UHPC) with efficient cement and mineral admixtures uses. *Cem. Concr. Compos.* 55, 383–394. doi:10.1016/j.cemconcomp.2014.09.024

Yu, R., Spiesz, P., and Brouwers, H. J. H. (2014). Mix design and properties assessment of ultra-high performance fibre reinforced concrete (UHPFRC). *Cem. Concr. Res.* 56, 29–39. doi:10.1016/j.cemconres.2013.11.002

Yu, R., Zhou, F., Yin, T., Wang, Z., Ding, M., Liu, Z., et al. (2021). Uncovering the approach to develop ultra-high performance concrete

(UHPC) with dense meso-structure based on rheological point of view: Experiments and modeling. *Constr. Build. Mater.* 271, 121500. doi:10.1016/j.conbuildmat.2020.121500

Yunsheng, Z., Wenhua, Z., and Zhengyu, C. (2017). Overview of ultra-high performance concrete: Design and preparation, microstructure, mechanics and durability, engineering applications. *Mater. Rep.* 31, 1–16.

Zerbino, R., Tobes, J. M., Bossio, M. E., and Giaccio, G. (2012). On the orientation of fibres in structural members fabricated with self compacting fibre reinforced concrete. *Cem. Concr. Compos.* 34 (2), 191–200. doi:10.1016/j.cemconcomp.2011.09.005

Zhang, P., Gao, Z., Wang, J., Guo, J., and Wang, T. (2022). Influencing factors analysis and optimized prediction model for rheology and flowability of nano-SiO2 and PVA fiber reinforced alkali-activated composites. *J. Clean. Prod.* 366, 132988. doi:10.1016/j.jclepro.2022.132988

Zhang, P., Han, X., Hu, S., Wang, J., and Wang, T. (2022). High-temperature behavior of polyvinyl alcohol fiber-reinforced metakaolin/fly ash-based geopolymer mortar. *Compos. Part B Eng.* 244, 110171. doi:10.1016/j.compositesb.2022.110171

Zhang, P., Wei, S., Wu, J., Zhang, Y., and Zheng, Y. (2022). Investigation of mechanical properties of PVA fiber-reinforced cementitious composites under the coupling effect of wet-thermal and chloride salt environment. *Case Stud. Constr. Mater.* 17, e01325. doi:10.1016/j.cscm.2022.e01325

Zhang, P., Wei, S., Zheng, Y., Wang, F., and Hu, S. (2022). Effect of single and synergistic reinforcement of PVA fiber and nano-SiO2 on workability and compressive strength of geopolymer composites. *Polymers* 14 (18), 3765. doi:10.3390/polym14183765

Zheng, Y., Zhuo, J., Zhang, P., and Ma, M. (2022). Mechanical properties and meso-microscopic mechanism of basalt fiber-reinforced recycled aggregate concrete. *J. Clean. Prod.* 370, 133555. doi:10.1016/j.jclepro.2022.133555